

Exploring the Frequency & Morphology of ErbB4-positive Cells in the Post-Mortem Brains of Schizophrenia Specimens: A Pilot Study

By Karina Di Pietro & John Badie



Art by Yixin Katherine Shan

Introduction

Schizophrenia (SZ) is a multifaceted neuropsychiatric disorder with several factors contributing to its onset. Clinicians use the 5th edition of the Diagnostic and Statistical Manual of Mental Disorders (DSM-V) to diagnose individuals with SZ based on the manifestation of several symptoms, such as delusions, hallucinations, catatonic behaviours, disorganized

speech, and declining cognitive and social function (McCutcheon et al., 2020). Schizophrenia has a strong neurobiological basis, with an 80% heritability rate. Despite high heritability, the precise etiology of SZ remains unclear. Virtually no SZ-linked genes exhibit patterns of Mendelian genetics, high penetrance, or significant odds ratios in association studies (Mei & Nave, 2014).

Understanding the intricate mechanisms underlying SZ involves examining key molecular players' roles, such as Erb-B2 Receptor Tyrosine Kinase 4 (ErbB4). ErbB4 is a receptor for neuregulin-1 (NRG-1), a protein that has been linked to schizophrenia (Law et al., 2006; Nicodemus et al., 2006). ErbB4 is a member of the ErbB family of receptor tyrosine kinases and has been implicated in various cellular processes, including glutamatergic synapse maturation, synaptic plasticity, and neuronal development (Li et al., 2007; Chen et al., 2010; Shamir et al., 2012). Roles of NRG-1 in the brain involve synapse formation, regulation of N-methylD-aspartate, GABA_A and acetylcholine receptor subunit expression and activity-dependent synaptic plasticity. Additionally, NRG-1 influences the proliferation, differentiation, and migration of various cell types, including Schwann cells (Law et al., 2004). The development of inhibitory circuits in the mammalian cortex is regulated by NRG1-ErbB4 signaling, which controls the connectivity of GABAergic interneurons through an ErbB4-dependent mechanism (Marenco et al., 2011). Maintaining optimal levels of NRG1-ErbB4 expression is essential for the

normal functioning of the adult brain; any deviation from the normal expression of NRG1-ErbB4 can lead to neurological impairment (Mei & Nave, 2014).

The genetic association between NRG1-ErbB4 and SZ is supported by most but not all studies (Mei & Nave, 2014). Some studies propose that abnormal NRG1-ErbB4 signaling affects the brain circuitry involving GABAergic interneurons, potentially explaining SZ symptoms (Joshi et al., 2014). Conversely, other studies suggest that upregulating ErbB4 may contribute to neurodegeneration and the progression of Alzheimer's Disease (AD), leading to psychosis and SZ. There is also uncertainty regarding the specific site of action where ErbB4 is believed to cause SZ. Further research and clinical trial replications are needed to gain a more comprehensive understanding of the roles of ErbB4-NRG1 in SZ (Joshi et al., 2014).

When considering schizophrenia's profound impact on individuals and society, exploring the association between ErbB4 and SZ becomes a crucial avenue for addressing the challenges posed by this disorder. SZ impacts individuals from all cultures, affecting around 1

percent of the population. The estimated average cost of a hospital stay for a Canadian patient with schizophrenia in 2017-2018 was \$12,971, the highest among all mental disorders (Stewart et al., 2022). Schizophrenia also has one of the highest mortality risks among psychiatric disorders (Correll et al., 2022). This neuropsychiatric disorder is linked to a notable reduction in life expectancy, with individuals affected facing a mean lifespan about 10-25 years shorter than the general population (Correll et al., 2022). Additionally, schizophrenic individuals have a 10% risk of suicide over their lifetime (Schultz et al., 2007). Investigating ErbB4's association with SZ can pave the way for improved treatments and early diagnostic measures. Such advancements could effectively address the health implications posed by SZ.

While existing studies have examined gene expression and protein levels related to schizophrenia in post-mortem brain tissues, the specific analysis of cellular parameters such as count, cell size and circularity, cortical orientation, and other spatial characteristics using *in situ* hybridization (ISH) data appears to be less explored. Currently, limited research focuses on the pat-

hways, localization of expression, and laminar differences in NRG1-ErbB4 expression between healthy adult brains and those with SZ. The present pilot study aims to address this gap by examining ErbB4 expression using ISH data from post-mortem tissues of three control subjects and three schizophrenic subjects. This study entails detailed analyses of ErbB4+ cell frequency, Feret angle, circularity, and distribution across cortical layers, specifically focusing on the right hemisphere of the dorsolateral prefrontal cortex (DLPFC). Based on the current literature concerning ErbB4 and SZ, we hypothesize a cellular difference exists in ErbB4-expressing cells in the dorsolateral prefrontal cortex when comparing control and schizophrenic (experimental) samples. We anticipate that there will be observable differences not only in the overall frequency of ErbB4-positive cells, but also in the morphological characteristics of the ErbB4-positive cells.

Methods

Tools Used for Data Processing & Analysis:

Raw data ISH expression images were obtained from the Allen Institute for Brain Science - Human

Brain Atlas. Image manipulation and analysis were performed using GNU Image Manipulation Program 2.10.36 (GIMP) and Fiji ImageJ version 2.14.0. Microsoft (MS) Excel version 16.80 was employed for statistical analysis and data visualization.

I. Raw Data Selection

Obtaining In-Situ Hybridization (ISH) Data (Allen Institute, 2013):

The current research utilized in situ hybridization (ISH) data sourced from the Schizophrenia Study in the Human Brain Atlas by the Allen Institute for Brain Science. Using colorimetric ISH methods, the Atlas provides cellular-level high-resolution gene expression information in specific brain regions (Allen Institute, 2013).

The Schizophrenia Study compares gene expression levels and patterns in the dorsolateral prefrontal cortex (DLPFC) between control and SZ groups (Figure 1). This study examined 60 genes, encompassing cell-type markers, cortical layer-specific markers, and SZ candidate genes, comparing control and SZ groups. The Allen Institute obtained the tissues for the Schizophrenia Study and the 1,000 Gene Survey in the Cortex from

post-mortem human subjects. The frozen post-mortem tissue samples were provided by the brain tissue collection of the Section on Neuropathology, Clinical Disorders Branch, GCAP, IRP, National Institute of Mental Health (NIMH), NIH in Maryland, USA. The subjects in these studies were adult male and female individuals, and the inclusion criteria required them to be at least 20 years of age. Control subjects for these studies had no known history of neuropsychiatric disease. The exclusion criteria for control subjects included evidence of drug use, suicide as the manner of death, and death due to drug overdose or poisoning. Rigorous inclusion and exclusion criteria ensured the quality of the samples, including checks for cerebellar pH, post-mortem interval (PMI), and confirmation of region of interest. Any samples with a pH less than 6 were excluded from this study. Smoking history (regular cigarette use) was categorized as "yes," "no," or "unknown" at the time of death, relying on information derived from medical records, family interviews, and nicotine levels. Ultimately, the study used specimens from 33 control and 19 SZ cases.

Our study focuses only on the

tissue samples dissected from DLPFC regions. Tissue qualification procedures confirmed the region of interest, RNA integrity, and absence of senile plaques and ice crystals. RNA extraction and quality assessment were performed using the MELT Total Nucleic Acid Isolation system and high-resolution capillary electrophoresis on an Agilent Bioanalyzer 2100, which generates RNA Integrity Numbers (RIN values). Higher RIN values indicate better RNA integrity. Various staining techniques were utilized to evaluate the presence of senile plaques and ice crystals, which, if identified in a sample, resulted in that sample's exclusion from further ISH procedures.

To perform ISH, post-mortem human brain tissue samples were harvested, sectioned into coronal slabs approximately 1 to 1.5 cm in thickness, and stored at -80°C until dissection. For the DLPFC, specific regions were dissected from the superior and middle prefrontal gyri, aiming to include Brodmann's areas 9 and 46 in each tissue block. DLPFC samples were predominantly sourced from the right cerebral hemisphere. Two image acquisition platforms were used to acquire and process high-resolution human cort-

ex visualizations: an automated microscopy platform and ScanScope scanners. The Informatics Data Pipeline (IDP) handles various processes such as image pre-processing, quality control, *ISH* expression detection, Nissl processing, and public data display. Since the IDP faced difficulties in handling large image sizes from human tissue sections, the Allen Institute migrated to a 64-bit Linux platform. Quality control measures were implemented after image acquisition and throughout data processing to ensure that only suitable images were available to the public.

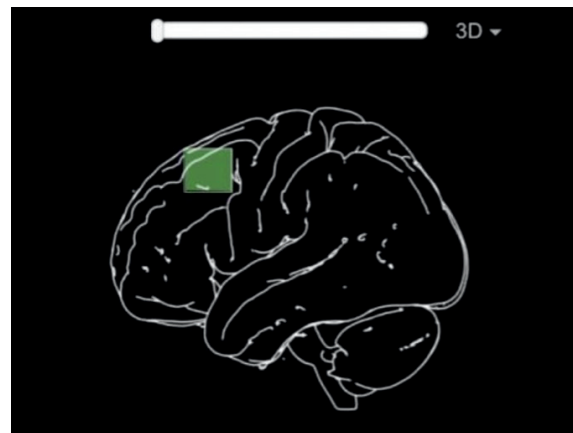


Figure 1. Dorsolateral Prefrontal Cortex. Illustrations depicting the regions of the dorsolateral prefrontal cortex that were removed and analyzed for gene expression using a colorimetric ISH method. These visualizations were created based on reference images generated by Dr. Jacopo Annese from The Brain Observatory at the University of California, San Diego.

ADVANCED TOPICS & ESSAYS

a. Sampling:

We utilized post-mortem brain tissue samples for three control and three SZ specimens from the Allen Brain Institute. All six specimens in our study were from the right hemisphere of the DLPFC. Nearly all six specimens were from non-smokers, except experimental specimen #3. Control specimen #1, identified by experiment number 80964005, featured a 20-year-old male donor. Control specimen #2 from experiment number 81354036, belonged to a 42-year-old male donor. Control specimen #3, identified by experiment number 81391472, was from a 34-year-old male donor.

For the experimental specimens: experimental specimen #1, marked by experiment number 81447989, featured a 42-year-old White male donor with SZ. Experimental specimen #2, linked to experiment number 81280947,

	Name(s)	Description	
Control Specimens	Control Specimen #1 (also referred to as Control #1)	Specimen ID: H08-0080 Experiment #: 80964005 Age: 20 years	Sex: male Race: White Smoking status: non-smoker
	Control Specimen #2 (also referred to as Control #2)	Specimen ID: H08-0101 Experiment #: 81354036 Age: 42 years	Sex: male Race: White Smoking status: non-smoker
	Control Specimen #3 (also referred to as Control #3)	Specimen ID: H08-0103 Experiment #: 81391472 Age: 34 years	Sex: male Race: White Smoking status: non-smoker
Experimental Specimens	Experimental Specimen #1 (also referred to as Experimental #1)	Specimen ID: H08-0122 Experiment #: 81447989 Age: 42 years	Sex: male Race: White Smoking status: non-smoker
	Experimental Specimen #2 (also referred to as Experimental #2)	Specimen ID: H08-0125 Experiment #: 81280947 Age: 34 years	Sex: male Race: African American Smoking status: non-smoker
	Experimental Specimen #3 (also referred to as Experimental #3)	Specimen ID: H08-0161 Experiment #: 81511768 Age: 22 years	Sex: male Race: White Smoking status: smoker

Table 1. Description of Specimens examined in the Present Study, obtained from the Allen Institute for Brain Science - Human Brain Atlas. Note: All six specimens in this study were sourced from the right hemisphere of the donor's DLPFC.

involved a 34-year-old female donor of African American ethnicity identified as having SZ. Lastly, experimental specimen #3, associated with experiment number 81511768, involved a 22-year-old White male smoker who also had SZ. Refer to Table 1 for a summary of each control and SZ donor, including their specimen ID, experiment number, age at time of death, sex, race, and smoking status.

We obtained our specimens from the Allen Brain Institute website, within the Allen Human Brain Atlas, subsequently selecting our gene of interest, ErbB4. We then added the 'ErbB4' experiment for each specimen to our selections, allowing us to launch the Allen Institute high-resolution image viewer, which provided access to the ISH, Nissl, and expression images for the chosen specimen and selected ErbB4 gene (Figure 2). Then, we downloaded the expression image as a JPEG with image quality set to 100 (Figure 2c).

To refine our expression image further, we used GNU Image Manipulation Program 2.10.36 (GIMP) to focus on a smaller sampling region. The samples were obtained and cropped in a manner that maintain-

ed layer 1 of the cortex at the top of the image and layer 6 at the bottom. Specifically, the sampling box was designed to incorporate Layer 1 by utilizing the easily recognizable pia mater as its upper boundary. After importing the ErbB4 expression image into GIMP, the Rectangle Select Tool was used to obtain a 1500:3000 sampling region just below the sulcus (Figure 2c). Following this, we copied the sampling region to our clipboard, then navigated to File and selected "Create from Clipboard," generating a new GIMP file containing the chosen rectangular area, which was subsequently saved as a JPEG (Figure 2d).

Certain images required rotation and straightening along the pia mater, specifically control specimen #1, control specimen #2, control specimen #3, and experimental specimen #2 (Figure 3). The process involved selecting a larger sampling window than described earlier, utilizing the Measure tool under "Tools" in the menu, dragging the Measure tool line along the desired top of the image, and clicking straighten to rotate the image along the line (Figure 4a-b). A 1500:3000 sampling region from the straightened/rotated image was chosen,

copied, and then a new GIMP file was created from the clipboard, followed by exporting the cropped expression image as a JPEG (Figure 4c-d).


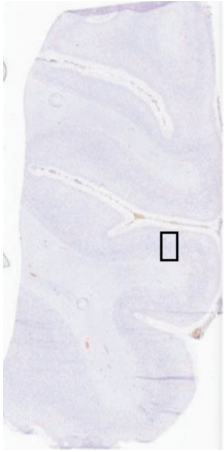

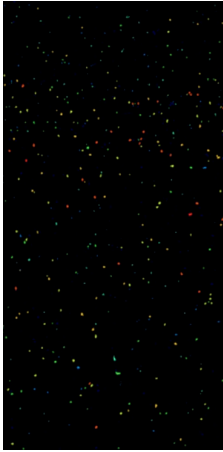
			
a) ISH	b) Nissl	c) Expression	d) Cropped expression image

Figure 2. Raw Data Selection from Allen Institute. a) In situ hybridization (ISH) data from Allen Institute for Experimental Specimen #1. b) Nissl stain from Allen Institute for Experimental Specimen #1. c) ErbB4+ expression image from Allen Institute for Experimental Specimen #1 d) Cropped expression image for Experimental Specimen 1, obtained using GNU Image Manipulation Program 2.10.36 (GIMP).

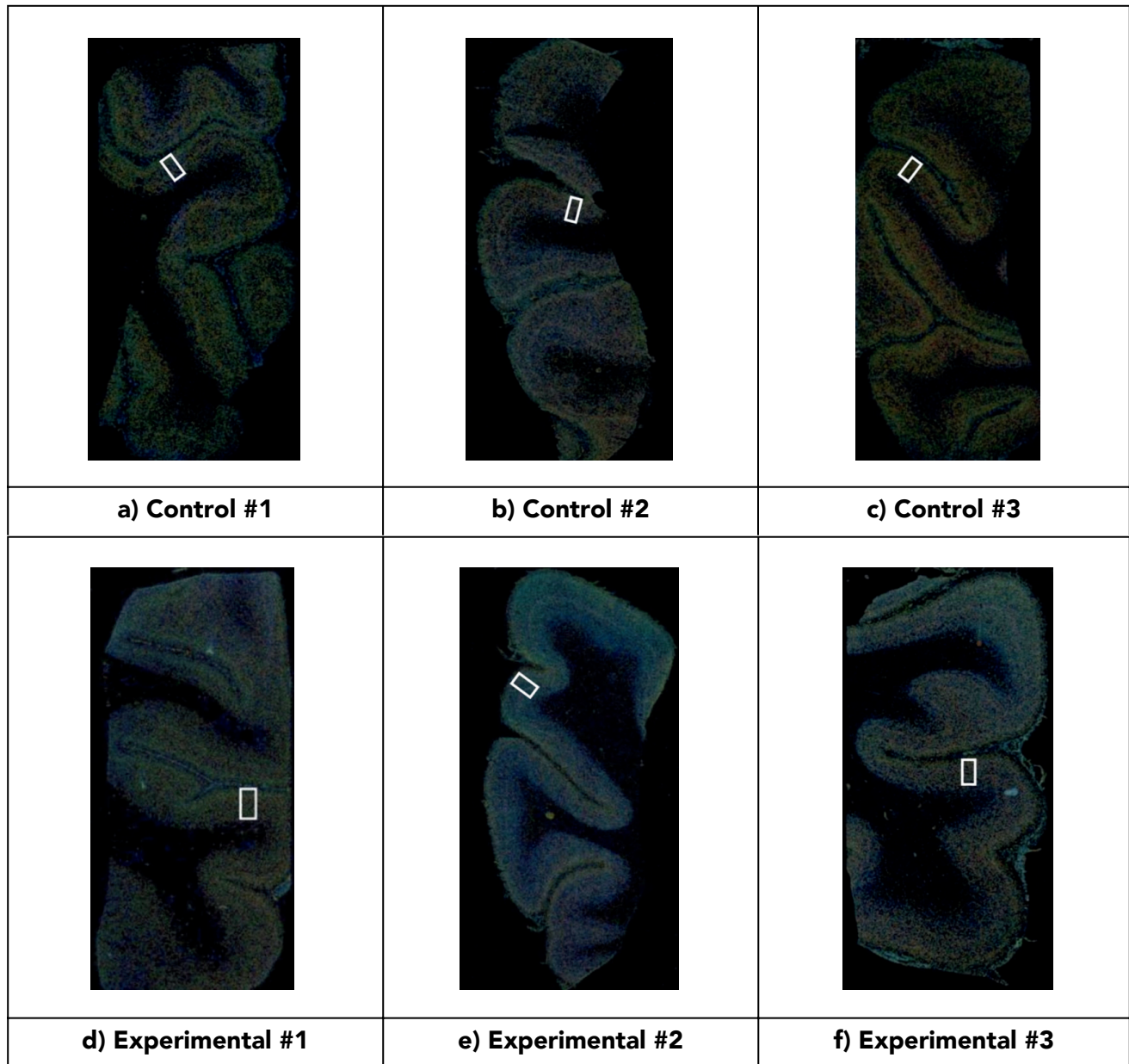


Figure 3. Selected Sampling Windows for All Six Specimens. Depiction of selected 1500:3000 sampling windows for each control and experimental specimen. a-d & f) Control specimens #1, #2, and #3, as well as Experimental specimens 1 and 3 were cropped directly below the sulcus. Control specimens #1, #2, and #3 were all cropped at non-right angles. Experimental specimens 1 and 3 were cropped at a right (90°) angle. e) Experimental specimen #2 was cropped more laterally at a non-right angle.

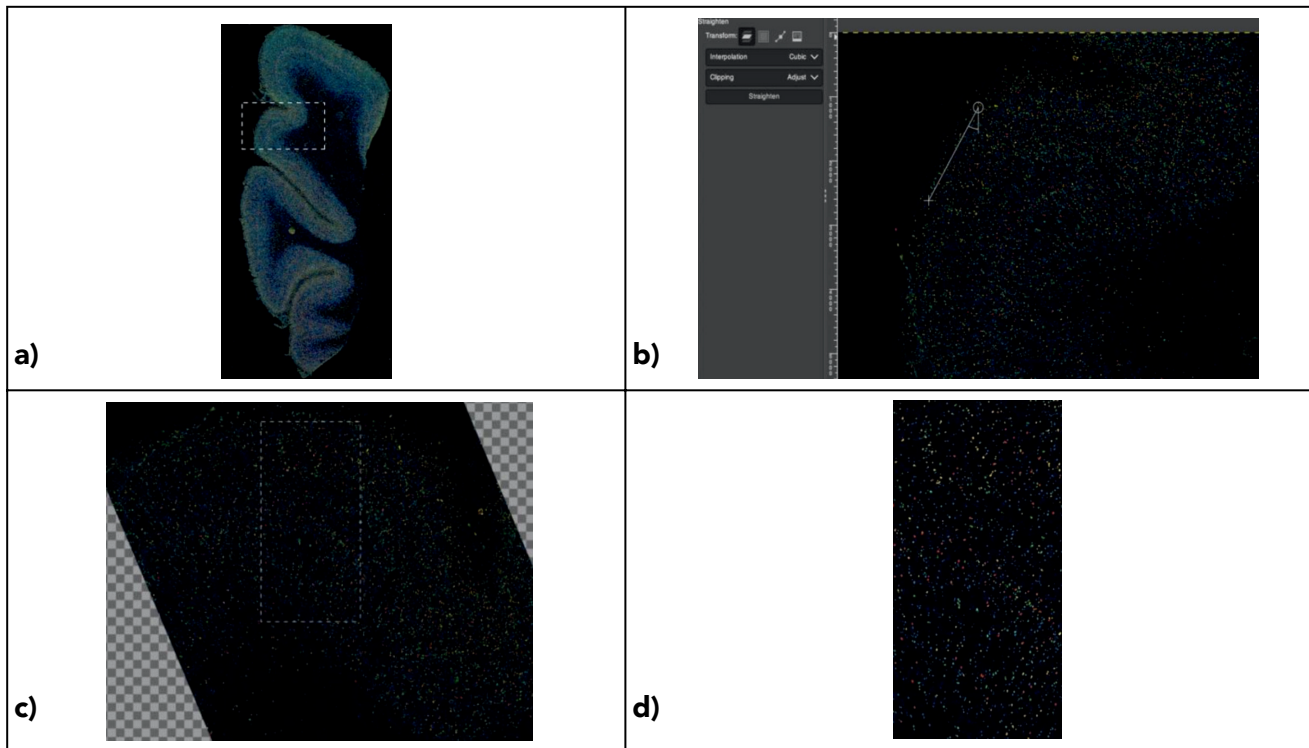


Figure 4. *Rotating Image along Pia Mater using GIMP.* Demonstrating rotation of ErbB4+ expression image using Experimental Specimen #2. a) Using Rectangle Select tool to select relatively big sampling region. b) Using the Measure tool to rotate the image along the pia mater. c) Selecting a cropped sampling region using the Rectangle Select tool. d) Final cropped ErbB4+ expression image for Experimental Specimen #2.

II. Cleaning of the Data

The cropped GIMP images were imported into Fiji ImageJ version 2.14.0 for particle analysis. In Fiji, each image was converted from Red, Green, Blue (RGB) colour model to 8-bit grayscale (Figure 5a). Under the Image menu, we adjusted the threshold by clicking "Adjust Threshold", and applying default settings, which disseminated the black background from the particles (Figure 5b). The scale was set to one pixel per micron, and using the "Set Measurements" function, we selected measurements for analysis to include area, minimum and maximum gray value, center of mass, shape descriptors, mean gray value, and Feret's diameter (Figure 5c-d).

III. Data Analysis

In Fiji, customized particle analysis settings, including "display results," "show outlines," "clear results," and "summarize," were applied using the "Analyze Particles" tool (Figure 5e). Circularity was set to 0.00 to 1.00, with a value of 1.0 indicating a perfect circle. To accommodate potential neural cell variations that might express ErbB4, the size range was set to 50-4000 micron² (μm^2). This lower limit of 50 μm^2 was used to filter out non-speci-

fic signals and debris from the ISH image analysis, as recommended by Dr. Kathryn Murphy during PNB 3L03 lectures. The particle analysis yielded a summary chart for all cells in the sampling window, a chart displaying data for individual cells, and a drawing showing the shapes and outlines of the cells within the specified sampling window (Figure 5f). The summary and results charts were exported as comma-separated files (CSV), and then opened with Micro-soft Excel.

Microsoft Excel version 16.80 was used to perform quantitative data analyses. The frequency of ErbB4+ cells throughout the cortex for control and experimental specimens was plotted based on cell size with a rolling window incremented by 75 μm on the x-axis. The rolling window represented depth into the cortex. "Small" cells were categorized as those whose area was less than or equal to 80 μm^2 and "large" cells included cells larger than 80 μm^2 . Cells larger than 80 μm^2 would represent parvalbumin-positive (PV+) interneurons, whose diameter averages 16 to 20 μm , and calretinin-positive interneurons, whose diameter ranges from 12 to 20 μm in diameter (Tepper & Koós, 2016). This is explained using πr^2 to

approximate the neuron's area given the specified diameter range 12-20 μm , which equates to 113 μm^2 -314 μm^2 . The specified range of 12-20 μm in diameter aligns with the average observed Feret diameter observed for our ErbB4+ cells expressed in controls and experimental samples: $17.22 \mu\text{m} \pm 0.75 \mu\text{m}$. The mean ErbB4+ cell count per individual specimen and per specimen type were also visualized using two bar graphs. The mean ErbB4+ cell count per specimen type was plotted a second time, with experimental specimen #2 excluded. Similar bar graphs were made to depict ErbB4+ cell count by cell size, on average. The mean proportion of small and large cells was plotted using a double-bar graph for control and experimental specimens.

In a similar manner, the frequency of ErbB4+ cells throughout the cortex for control and experimental specimens was plotted based on cell circularity with a rolling window incremented into 75 μm on the x-axis. The "low circularity" label included cells less than or equal to 0.30, "moderate circularity" was indicative of cells greater than 0.30 but less than 0.80, and "high circularity" was representative of

cells greater than or equal to 0.80 on a scale from 0.00 to 1.00, where 1.00 represents a perfect circle. A double-bar graph was used to show the mean proportion of high, moderate, and low circularity cells per specimen type. Another bar graph showed the average cell circularity value per specimen type.

Lastly, MS Excel was used to assess the frequency of various Feret angles for ErbB4-positive cells in control and experimental specimens. A Feret angle frequency distribution was created for all six specimens, utilizing nine bins, each spanning twenty degrees. The total range covered was from 0 to 180 degrees. A similar frequency distribution with the same nine bins was plotted for the mean frequencies of Feret angles across control and experimental specimens. A summary bar graph was also produced, depicting the mean Feret Angle for control and experimental specimens.

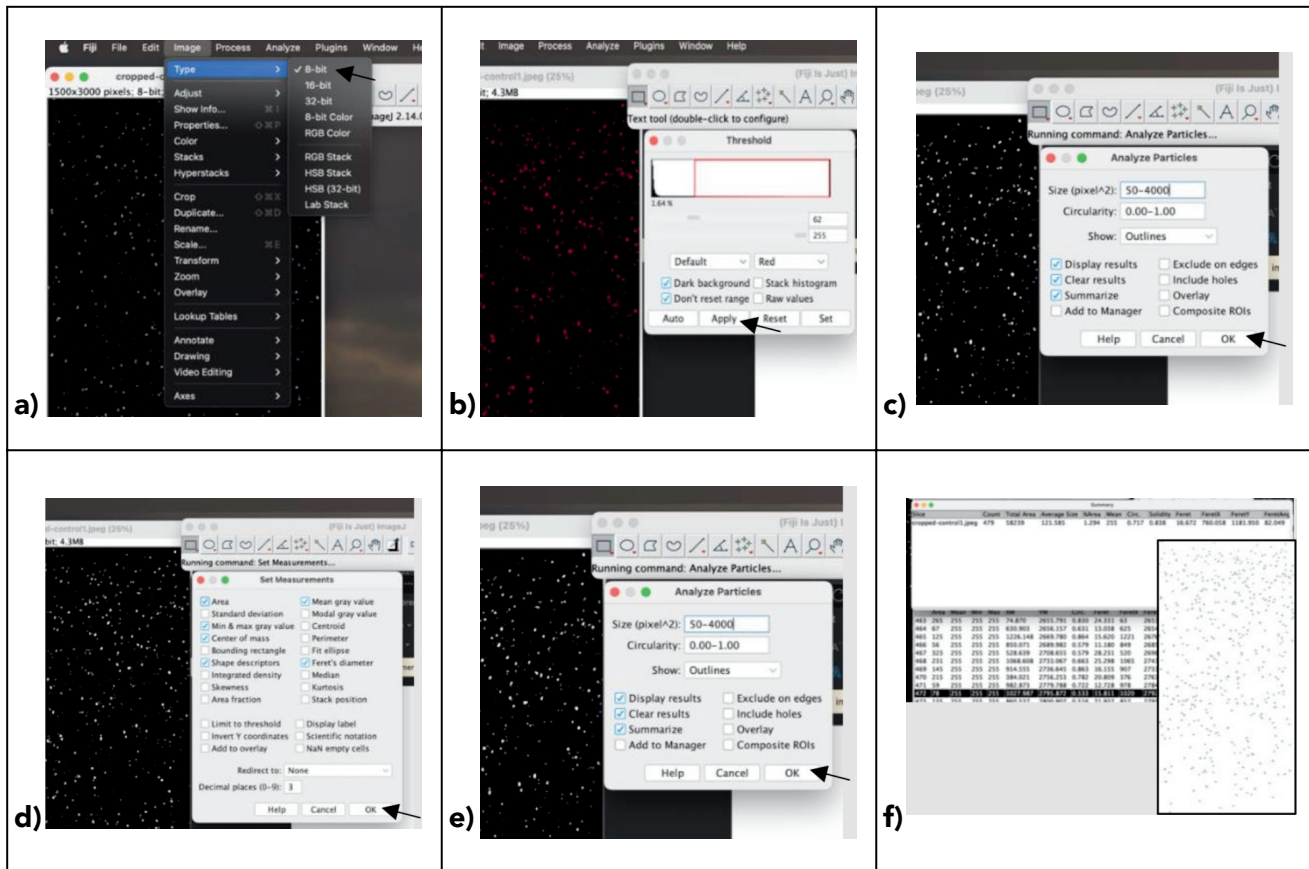


Figure 5. How data was extracted and analyzed in Fiji. a) Setting JPEG image from GIMP to 8-bit grayscale in Fiji (ImageJ). b) Setting threshold to default settings. c) Setting scale to 1 pixel per micron. d) Setting measurements: area, minimum and maximum gray value, center of mass, shape descriptors, mean gray value, Feret's diameter. e) Analyzing particles that have an area between 50 to 4000 μm^2 , with a circularity between 0.00 and 1.00. f) Product of particle analysis: black and white drawing, results CSV, summary of mean values for count, average cell size in microns squared, circularity, Feret angle, x- and y-position.

Results

I. Qualitative Analysis

ErbB4 expression can be observed in all six layers of the cortex, with varying levels in each layer (Figure 6). Observing the cropped ErbB4+ expression images with the naked eye shows us that there appears to be noticeably higher lev-

els of ErbB4+ cells in all layers of experimental sample #2, compared to all other control and experimental specimens (Figure 6). On the contrary, control specimens #1 and #2 appear to have higher levels of ErbB4 expression than experimental specimens #1 and #3 (Figure 6). Control specimen #3 and experime-

ntal specimens #1 and #3 appear to have similar levels of ErbB4 expression (Figure 6 & Figure 7). Overall, it seems that if we exclude experimental specimen #2 from our statement, control specimens have greater levels of ErbB4 expression than experimental samples.

By examining the expression and Nissl images in isolation, we could not qualitatively assess cell size, circularity, Feret angle, and Feret diameter for ErbB4+ positive cells from direct observation. Furthermore, we were also unable to visually assess differences across control and experimental samples for the frequency of ErbB4+ cells in each of the six cortical layers. However, we see that, for all samples, the lower layers (layers 5 & 6) and uppermost layer (layer 1), have lower levels of ErbB4 expression than the middle layers (layers 2-4) as indicated by the elevated densities of red cells in these regions (Figure 6 & Figure 7). This observation also corresponds to a slightly darker region of cells in the middle layers of the Nissl stain images from the Allen Institute website (Figure 8).

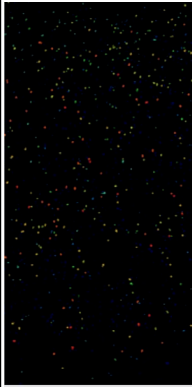
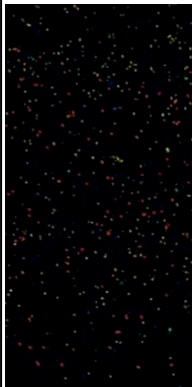
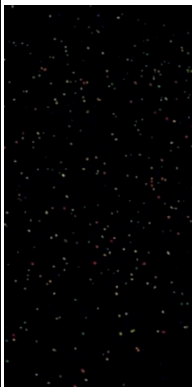
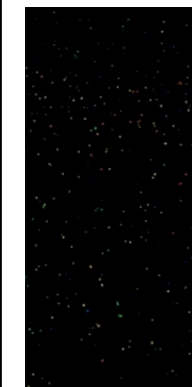
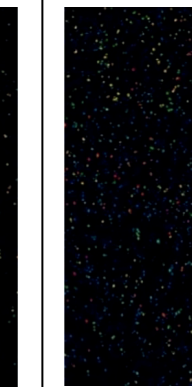
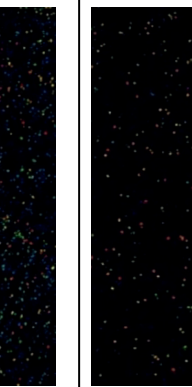
					
a) Control Specimen #1	b) Control Specimen #2	c) Control Specimen #3	d) Experimental Specimen #1	e) Experimental Specimen #2	f) Experimental Specimen #3

Figure 6. ErbB4+ expression images from the Allen Institute Human Brain Atlas. Expression images were cropped using GNU Image Manipulation Program 2.10.36 (GIMP). ErbB4 expression levels are indicated by different colors, with red denoting the highest ErbB4 expression level, followed by yellow and orange, then green, and finally blue indicating the lowest ErbB4 expression level. a) Control Specimen #1; b) Control Specimen #2; c) Control Specimen #3; d) Experimental Specimen #1; e) Experimental Specimen #2; f) Experimental Specimen #3.





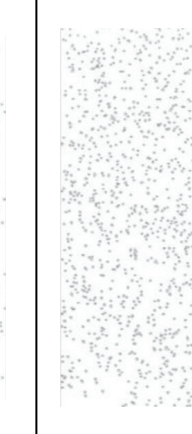
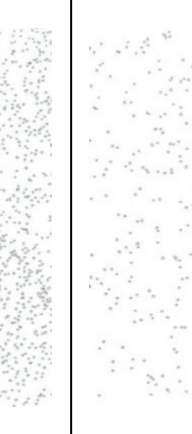
					
a) Control Specimen #1	b) Control Specimen #2	c) Control Specimen #3	d) Experimental Specimen #1	e) Experimental Specimen #2	f) Experimental Specimen #3

Figure 7. Drawings of ErbB4+ Cells for Each Specimen. a) Control Specimen #1; b) Control Specimen #2; c) Control Specimen #3; d) Experimental Specimen #1; e) Experimental Specimen #2; f) Experimental Specimen #3 exported from Fiji (ImageJ) analysis.

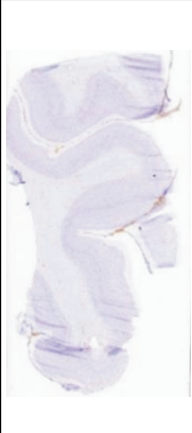



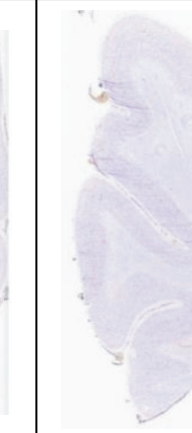
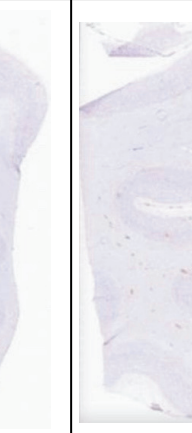
					
a) Control Specimen #1	b) Control Specimen #2	c) Control Specimen #3	d) Experimental Specimen #1	e) Experimental Specimen #2	f) Experimental Specimen #3

Figure 8. Nissl stain of ErbB4+ cells for Each Specimen. a) Control Specimen #1; b) Control Specimen #2; c) Control Specimen #3; d) Experimental Specimen #1; e) Experimental Specimen #2; f) Experimental Specimen #3 exported from the Allen Institute website.

II. Quantitative Analysis

Cell Count for ErbB4+ Cells in Control vs. Schizophrenic Donors

When comparing the mean Erb-

B4+ cell count for all three control donors and all three experimental donors, there was a 39.1% increase from the control specimen mean,

478 ErbB4+ cells, to the experimental sample mean of 664 ErbB4+ cells (Figure 9b). However, it is worth noting that this data is skewed heavily by experimental sample #2 (Figure 9a). The ErbB4+ cell count for experimental sample #2 was 1359, which was a 128.403% increase from the ErbB4+ cell count of 595 for control sample #2 (Figure 9a). Control specimens #1, #2, and #3 had higher ErbB4+ cell counts than experimental specimens #1 and #3 (Figure 9a). When excluding experimental specimen #2 from our analyses, we see a different trend, whereby there is a 24.3% decrease in cell count from control samples (mean = 419) to experimental samples (mean = 317) (Figure 9c). With experimental specimen #2 excluded, the range in ErbB4+ cells for experimental specimens decreases significantly, from 1055 to 26.

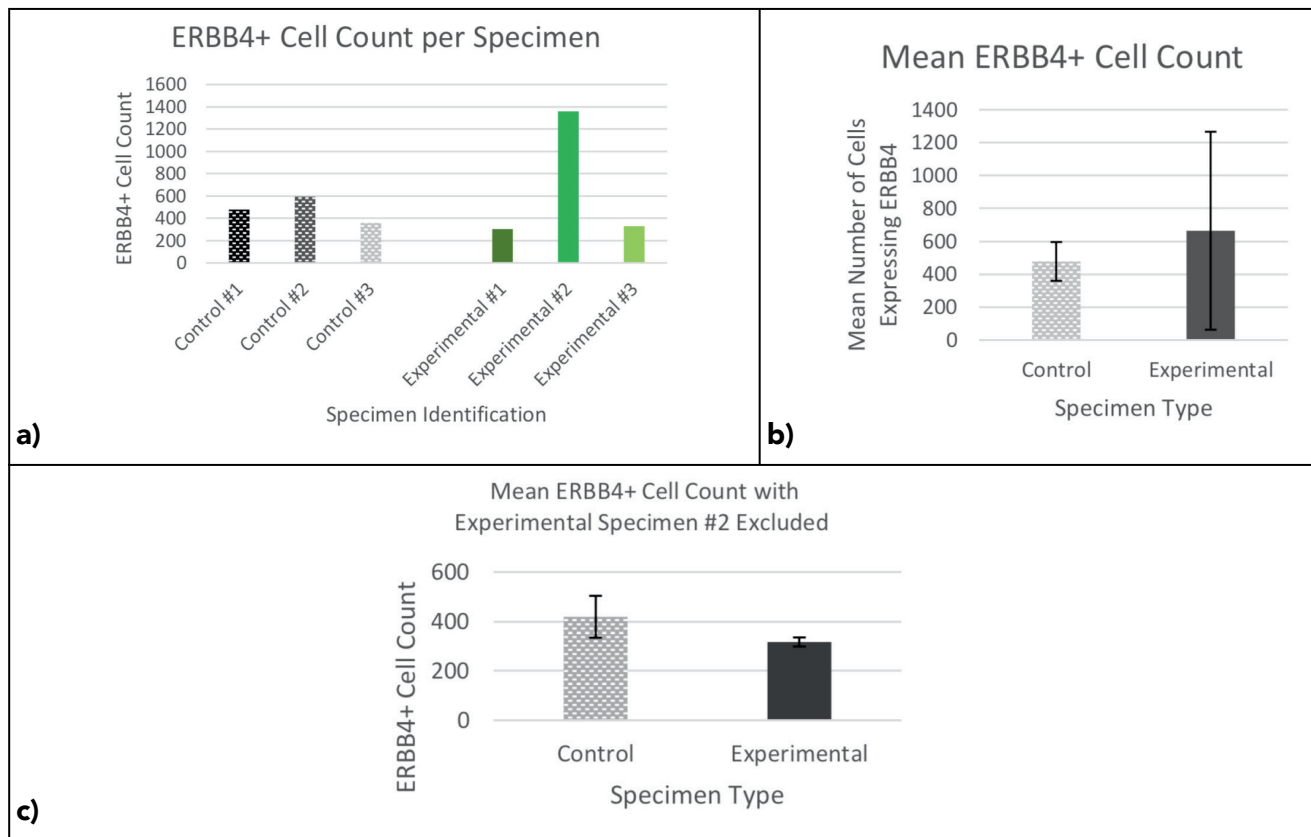


Figure 9. Cell Count for ErbB4+ Cells in Control vs. Schizophrenic Donors. a) ErbB4+ cell counts for each of the six specimens. b) Mean ErbB4+ cell counts for control specimens (N=3, mean=478 ± 118) and experimental specimens (N=3, mean=664 ± 602). c) Mean ErbB4+ cell counts for control specimens (N=2, mean=419 ± 85) and experimental specimens (N=2, mean=317 ± 18) with experimental specimen #2 and control specimens #2 excluded from calculations.

Cell Count by Size for ErbB4+ Cells in Control vs. Schizophrenic Donors

Control and experimental specimens have similar proportions of large ($> 80 \mu\text{m}^2$) and small ($\leq 80 \mu\text{m}^2$) ErbB4+ cells (Figure 10a). However, on average, control specimens have a 6% higher proportion of large cells than experimental specimens. Conversely, experimental specimens show a 7% higher proportion of small cells than control specimens.

The mean cell size for the control specimens was greater than that of the experimental specimens, when averaged across the three control specimens and three experimental specimens (Figure 10b). Specifically, the mean cell size (μm^2) for control specimens increased by 12.7% when compared to that of the experimental specimens (Figure 10b). The average cell size for control specimens was $137.3 \mu\text{m}^2$ which falls into the large cell size category. The average cells size for experimental specimens was $121.8 \mu\text{m}^2$, which also falls into the large cell size category.

As stated in the qualitative analysis, it looks like ErbB4 is expressed, to varying degrees throughout all six layers of the cortex (Figure 10c-f). Experimental specim-

ens consistently express a higher frequency of small ErbB4+ cells than control specimens (Figure 10e). At approximately $350 \mu\text{m}$, and $1750 \mu\text{m}$, there is a peak in the laminar analysis for large ErbB4+ cells in control specimens, that surpasses the frequency of large ErbB4+ cells in experimental specimens at the same x-axis value (Figure 10f). Apart from these specified differences, however, the frequency of ErbB4+ expression in cells any size throughout the cortex is distributed very similarly between control and SZ samples, with higher frequencies for ErbB4 expression in the middle and upper layers, and less ErbB4 expression in the lower layers (5 and 6) (Figure 10e-f). Between the depths of $2250 \mu\text{m}$ to $3000 \mu\text{m}$ into the cortex, a noticeable disparity was observed in the mean frequency of small ErbB4+ cells between the experimental and control specimens, with the former exhibiting a higher frequency (Figure 10e). Similarly, between the depths of $1900 \mu\text{m}$ to $3000 \mu\text{m}$, a pronounced difference was observed in the mean frequency of large ErbB4+ cells between the two groups, with the experimental specimens showing a higher frequency (Figure 10f). Overall, experimental specimens have

greater expression of ErbB4 in the lower layers than control specimens. For a detailed visualization of ErbB4+ cell count by size for each of the six specimens, refer to Figure 10c, d.

Cell Circularity for ErbB4+ Cells in Control vs. Schizophrenic Donors

On average, the mean proportion of total cells that are high circularity (≥ 0.80) is greater for experimental than control specimens, but only by a difference of 6.7% (Figure 11a). Control specimens have a notably higher mean percentage of moderately circular cells (>0.30 , <0.80), showing a 53% increase from the experimental specimens (Figure 11a). The proportion of low circularity (≤ 0.30) ErbB4+ cells for both control and experimental specimens was below 1% (Figure 11a). Overall, the mean values for circularity for control and experimental specimens are extremely similar, differing only by less than one-tenth (Figure 11b). Experimental specimens show a similar distribution of ErbB4+ cells for those with high and moderate circularity as depth into the cortex increases (Figure 12d, f). Tissues from SZ donors show a decrease in frequency of ErbB4+ cells as depth

into the cortex increases, with a sudden decrease at 1425 μm for moderate circularity cells and around 1200 μm for high circularity cells (Figure 12d, f). Tissues from control donors show a bimodal frequency distribution for moderate circularity ErbB4+ cells, whereby the upper layers of the cortex (i.e. 75 microns to 675 microns) and the lower-middle layers (i.e. 1575 microns to 1900 microns) have the highest ErbB4+ cell count (Figure 12d). A peak is seen for the control specimen between 1500 μm and 1800 μm when looking at high circularity ErbB4+ cell frequency (Figure 12f). Apart from this peak, the rest of the control ErbB4+ high circularity cell count is lower than that of the experimental specimen (Figure 12f). For an in-depth visualization of ErbB4+ cell count by circularity level for each of the six specimens, refer to Figure 12a, c, e.

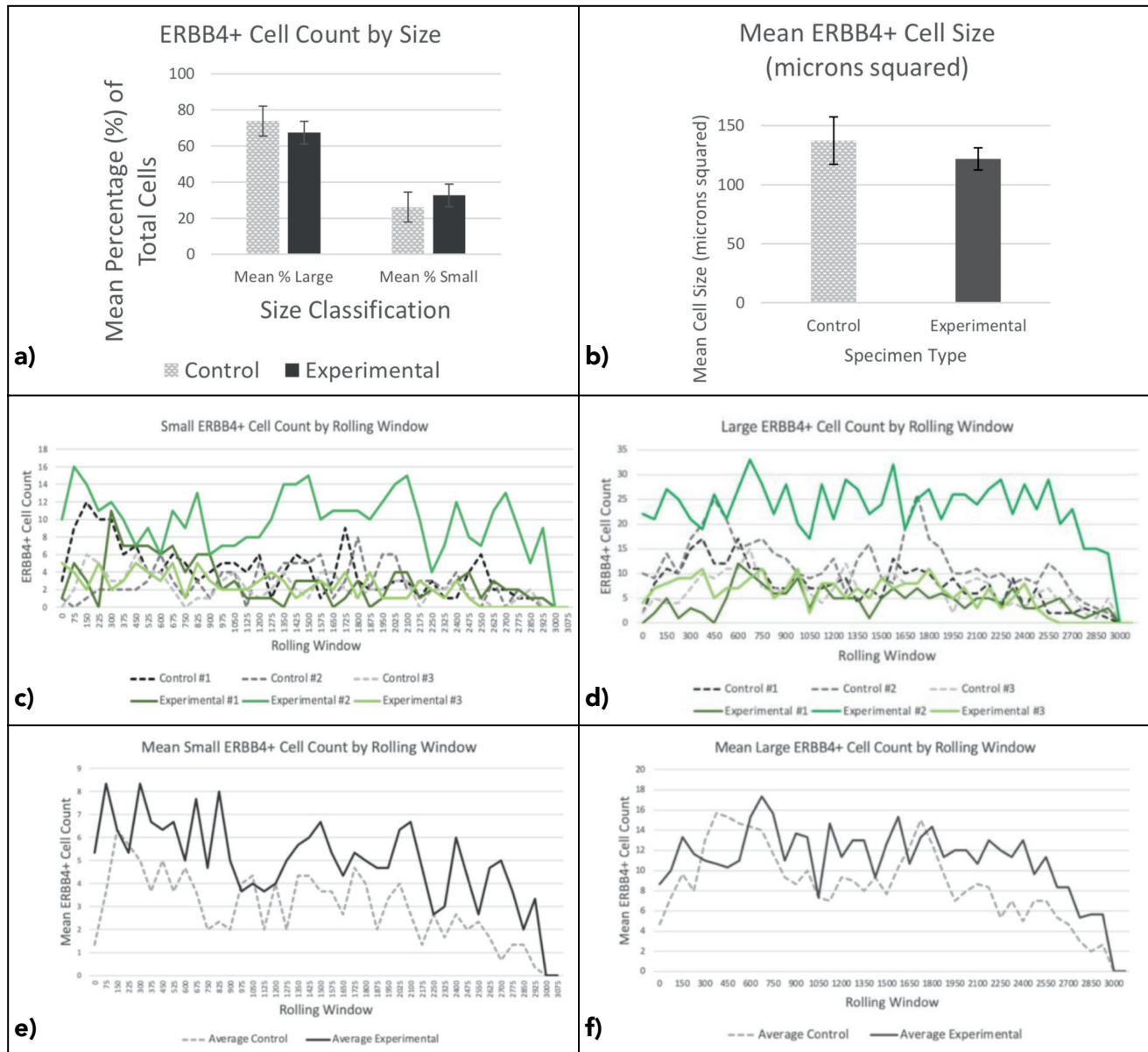


Figure 10. Cell Count by Size for ErbB4+ Cells in Control vs. Schizophrenic Donors. Large cells are $> 80 \mu\text{m}^2$, small cells are $\leq 80 \mu\text{m}^2$. a) Comparing the mean % of total cells that are categorized as Small or Large for control (mean % large = 73 ± 8.3 , mean % small = 26 ± 8.3) and experimental (mean % large = 67 ± 6.3 , mean % small = 33 ± 6.3). b) Comparing the mean cell size (μm^2) for control specimens (N=3, mean= 137.3 ± 20.1) and experimental specimens (N=3, mean= 121.8 ± 9.3). c) Small (area $\leq 80 \mu\text{m}^2$) ErbB4+ cell count by rolling window for each specimen (N=6), where the x-axis increases by increments of $75 \mu\text{m}$ (depth into the cortex). d) Large (area $> 80 \mu\text{m}^2$) ErbB4+ cell count by rolling window for each specimen (N=6). e) Mean small (area $\leq 80 \mu\text{m}^2$) ErbB4+ cell count for control (N=3) and experimental specimens (N=3) by rolling window. f) Mean large (area $> 80 \mu\text{m}^2$) ErbB4+ cell count for control (N=3) and experimental specimens (N=3) by rolling window.

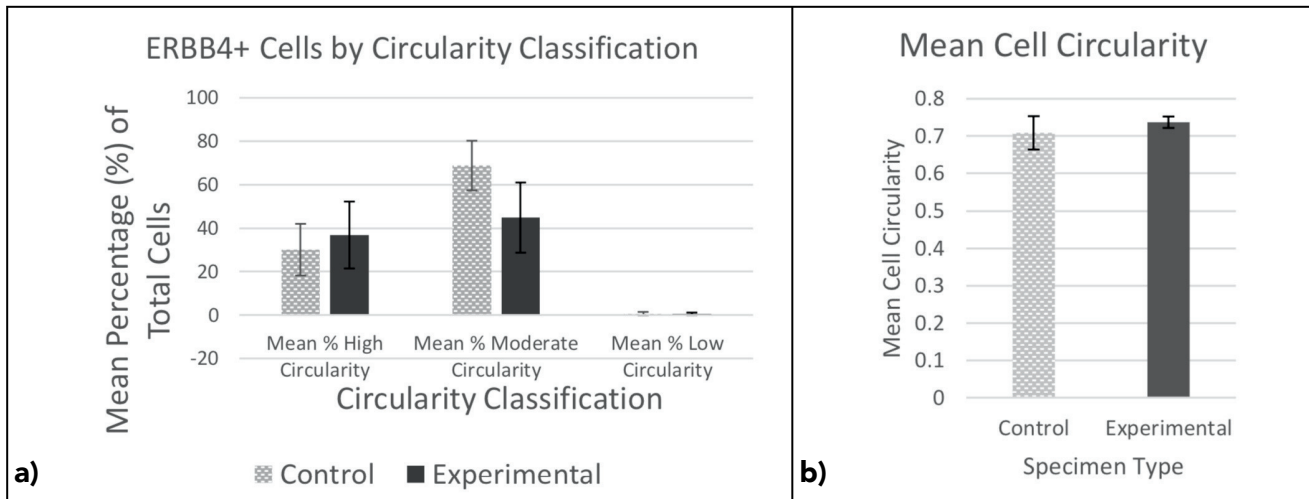


Figure 11. Summary of Cell Circularity for Control vs. Schizophrenic Donors. a) Comparing the mean % of total cells that are categorized as high circularity (≥ 0.80), moderate circularity (> 0.30 , < 0.80) or low circularity (≤ 0.30). for control (mean % high circularity = 30.1 ± 11.9 , mean % moderate circularity = 68.8 ± 11.4 , mean % low circularity = 0.64 ± 0.78) and experimental (mean % high circularity = 36.8 ± 15.4 , mean % moderate circularity = 44.9 ± 16.2 , mean % low circularity = 0.563 ± 0.570). b) Comparing the mean value for cell circularity for control (N=3, mean = 0.709 ± 0.045) and experimental (N=3, mean = 0.737 ± 0.015).



Figure 12. Cell Count by Circularity for ErbB4+ Cells in Control vs. Schizophrenic Donors across Rolling Window. The “low circularity” label included cells ≤ 0.30 , “moderate circularity” was indicative of cells > 0.30 but < 0.80 , and “high circularity” was representative of cells ≥ 0.80 on a scale from 0.00 to 1.00, where 1.00 represents a perfect circle. a) Low circularity ErbB4+ cell count by rolling window for each specimen (N=6), where the x-axis increases by increments of 75 μm (depth into the cortex). b) Mean low circularity ErbB4+ cell count for control (N=3) and experimental specimens (N=3) by rolling window. c) Moderate circularity ErbB4+ cell count by rolling window for each specimen (N=6) with rolling window as the x-axis. d) Mean moderate circularity ErbB4+ cell count for control (N=3) and experimental specimens (N=3) by rolling window. e) High circularity ErbB4+ cell count by rolling window for each specimen (N=6) with rolling window as the x-axis. f) Mean high circularity ErbB4+ cell count for control (N=3) and experimental specimens (N=3) by rolling window.

Assessing Feret Angle of ErbB4+ Cells in Control vs. Schizophrenic Donors

The average Feret angle for control specimens is 102° , compared to a mean Feret angle of 86° for experimental specimens (Figure 13a). When analyzing frequency distributions plotting ErbB4+ cell count against Feret angle for control and experimental donors across nine bins increasing by 20-degree increments, experimental specimens consistently have greater frequencies of ErbB4+ cells from 0° to 120° and control specimens have greater ErbB4+ cell counts for Feret angles $>120^\circ$ (Figure 13b, c).

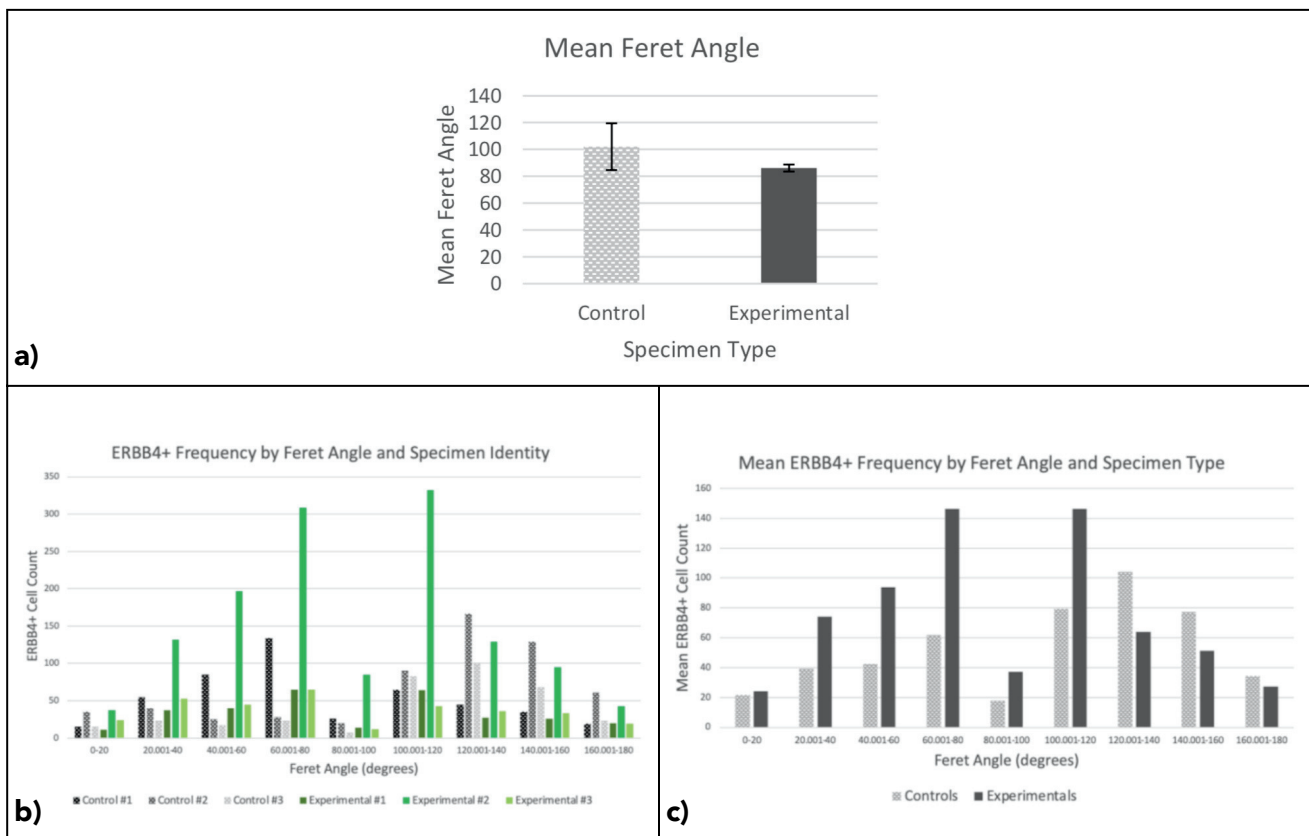


Figure 13. Analysis of Feret Angle ($^\circ$) Frequencies for Control and Schizophrenic Donors. a) Mean Feret Angle vs. Specimen Type: control (N=3, mean= $102^\circ \pm 17.4$) and experimental (N=3, mean= $86^\circ \pm 2.6$). c) Frequency distribution of Feret Angle (0 - 180°) for all six specimens utilizing nine bins, each spanning 20° . d) Frequency distribution of mean ErbB4+ cell count by Feret Angle and Specimen Type (control or experimental) utilizing nine bins, each spanning 20° .

Discussion

Our study aimed to investigate the expression patterns of ErbB4 in the post-mortem brains of schizophrenic donor samples and compare them to control donor samples. To achieve this, we conducted a qualitative analysis of ErbB4 expression across all six layers of the cortex using images obtained from the Allen Institute Human Brain Atlas. Additionally, a quantitative analysis was carried out to quantify ErbB4+ cell frequency, cell size (μm^2), circularity, and measurement of Feret angles. Overall, the findings support our hypotheses and expectations, highlighting differences in ErbB4 expression and morphology between control and experimental specimens, with variations in cell count, size, circularity, and Feret angle.

ErbB4 Expression Frequency

Both quantitative and qualitative analyses demonstrated that ErbB4 is expressed in all six layers of the cortex, with varying levels in each layer for both control and SZ donor samples. One of our primary findings was that control specimens generally exhibit higher levels of ErbB4 expression than experimental specimens, except for experimental

specimen #2. While our observations for experimental specimen #2 having much higher ErbB4 expression levels than non-schizophrenic individuals align with the widespread literature on the topic, the observed general decrease in ErbB4 levels from controls to experimental specimens contradicts popular findings. For instance, Joshi et al. (2014) reported elevated ErbB4 mRNA expression in layers 1, 2 and 5 of the prefrontal cortex of SZ subjects, suggesting the involvement of ErbB4 in these specific cortical layers. Another investigation has suggested that SZ-associated NRG1 and ErbB4 mRNA elevations also occur at the protein level and may be specific to SZ (Chong et al., 2008). The disparities between our study and these major findings might be explained by the known effects of loss of ErbB4 signaling: reduced oligodendrocyte number and morphology, thinner myelin, and slower conduction velocity in CNS axons (Roy et al., 2007). Transgenic mice with dampened ErbB4 levels exhibit increased dopamine receptors and transporters, along with behavioural alterations consistent with neuropsychiatric disorders (Roy et al., 2007). These biological effects of

disrupted ErbB4 signaling align with our observation of decreased ErbB4 expression in SZ subjects, providing a potential mechanistic explanation for the differences in ErbB4 levels between control and experimental specimens in our study.

ErbB4 Distribution throughout Cortical Layers

When we include experimental specimen #2 in our analysis, calculating average ErbB4 expression across the three control donors and three SZ donors, our mean values reflect the current literature that associates SZ with elevated ErbB4 expression. Also consistent with previous findings, when comparing the mean ErbB4 expression in control and experimental donors, we found that layers 1, 2 and 5 showed higher ErbB4 expression in SZ samples (Joshi et al., 2014). This supports the suggestion that dysregulation of ErbB4 in cortical layers 1, 2 and 5 of SZ individuals may be related to alterations in the function or density of specific neuronal subtypes present in these layers.

There is minimal research looking at the size differences in ErbB4+ cells throughout the cortical layers. However, it has been found that the

loss of ErbB4 signaling has been linked to changes in oligodendrocyte number and morphology, reduced myelin thickness, and altered white matter connectivity in the frontal and temporal lobes, which are regions implicated in SZ (Konrad et al., 2008). Our study builds upon the morphology-related findings of Konrad et al. by revealing that experimental samples consistently exhibit a greater prevalence of ErbB4+ cells of smaller size, while control samples consistently exhibit a higher frequency of larger ErbB4+ cells. Controls having larger ErbB4+ cells could signify enhanced cell growth or division, while experimental samples having higher frequencies of small ErbB4+ cells may suggest cell immaturity and altered proliferation dynamics.

Circularity

While differences in ErbB4+ cell circularity were observable, they were not drastic. Despite the subtlety of the changes, a consistent trend emerged, revealing that experimental specimens, on average, displayed a higher incidence of cells with elevated circularity compared to the control group. Control specimens had a higher mean frequency of moderately circular cells. The

higher incidence of cells with elevated circularity in experimental specimens implies that the presence or absence of ErbB4 may influence the overall shape of cells. The findings parallel existing research on the functional consequences of ErbB4 ablation in excitatory neurons, particularly the reduction in dendritic spine density within the prefrontal cortex (Cooper & Koleske, 2014). The interplay between ErbB4 expression, dendritic spine density, and cell circularity indicates a complex regulatory mechanism. This complexity implies that the effects of ErbB4 on cellular morphology are part of a broader network of signaling pathways and molecular interactions.

Feret Angle

As discussed in lecture, the orientation of a neuron's dendrites and axon in the prefrontal cortex can impact communication within and between layers, as well as along the surface of the cortex. Currently, there are no studies that investigate the Feret angle of ErbB4+ cells. The Feret angle (0-180°) is the angle between Feret's diameter and a line that runs parallel to the x-axis of the image (Ferreira & Rasband, 2012). A 90° angle would facilitate communi-

cation between the cortical layers, while a 0°-20° or 160°-180° degree angle would promote communication within a single layer. A 45° or 145° angle would represent an intermediate orientation, allowing for a potential combination of communication within and between layers. Control specimens were found to have a higher mean Feret angle than experimental specimens. Frequency distributions showed that experimental specimens consistently have greater frequencies of ErbB4+ cells for Feret angles from 0 degrees to 120 degrees, with the highest peaks between 60°-80° and 100°-120°. This suggests a predominant orientation of ErbB4+ cells in experimental specimens towards angles that are conducive to communication between the six cortical layers. Meanwhile, control specimens have greater frequencies for Feret angles >120 degrees, with the highest peak from 120°-140°. Hence, control specimens seem to have ErbB4+ cells in orientations that could promote between and within-layer cell-to-cell communication.

Strengths & Limitations

The major strength of this study lies in the unparalleled quality of the

images from the Allen Institute database, setting it apart as an exceptional resource with few equivalents worldwide. The Allen Institute's Human Brain Atlas is renowned for its exceptional quality due to several factors. Firstly, the institute employs cutting-edge neuroimaging technologies, such as MELT Total Nucleic Acid Isolation system and high-resolution capillary electrophoresis to capture detailed visualizations of the human brain with unprecedented clarity (Allen Institute, 2013). Additionally, the Allen Institute is committed to several stages of thorough quality control measures to ensure accuracy and reliability.

While Allen Institute has provided us with detailed brain scans for analysis, the quality and cost of the brain scans also limited the quantity and characteristics of the samples. It was difficult to control for age, sex, race, and smoking status between Schizophrenic and control samples due to the limited amount of available brain scans. For example, our samples did not consistently represent one race or ethnicity (White, N=5, African American, N=1), and one of our experimental specimens was a smoker (N=1) whereas the remain-

ing five were non-smokers. Additionally, we had an imbalanced sex distribution, with one sample from a female donor (experimental specimen #2), and the other five from males. Sex differences are important to consider, since the onset of SZ is often later in women than in men (Schultz et al., 2007). As such, these individual differences may add some noise and reduce the generalizability of the experiment results but are not significant enough to compromise the validity of our current pilot study, which aims to explore the ErbB4 dynamics within the post-mortem brain tissues of control versus SZ donors. Additionally, only the DLPFC was available to study among all patients concerning ErbB4, limiting our ability to assess and contrast the sites of localization of ErbB4 expression between SZ and control samples. However, studying the DLPFC provided significant insights pertaining to ErbB4 expression and how this expression plays a role in the ErbB4 pathways of SZ etiology.

Future Research Directions

It is important to note that this present investigation is a pilot study and while it brings forth valuable information and evidence concern-

ing ErbB4 expression discrepancies between schizophrenic and control donor samples, more research must be conducted to corroborate these findings. Future studies should look to incorporate larger sample sizes to increase the power and reliability of our experimental results, thereby decreasing susceptibility to outliers.

Additionally, the complexity of ErbB4's function obscures the site where it is active in SZ. Future studies should collect and contrast ErbB4 expression from multiple ErbB4-expressing regions of the brain, such as the hippocampus, basal forebrain, visual cortex, and prefrontal cortex to comprehensively assess if there are trends in expression correlating to SZ prognosis (Corfas et al., 1995; Neddens & Buonanno, 2011; Woo et al., 2011).

There is ongoing debate regarding whether the expression of ErbB4 provides a protective or adaptive function for individuals with SZ and Alzheimer's disease (AD). Some studies have mentioned that ErbB4 expression helps mitigate brain deterioration and mediates GABAergic interneuron function (Woo et al., 2011), which contradicts the previously mentioned findings of increased ErbB4 expression in SZ

samples. Moreover, studies in transgenic mice models with mutations in Amyloid precursor protein and Presenilin genes have shown elevated expressions of NRG1-ErbB4. These proteins, associated with the production of beta-amyloid neuritic plaques, are implicated in the neurodegenerative process in AD (Woo et al., 2011). By manipulating ErbB4 expression in mammalian brains, researchers may uncover insights into the association between ErbB4 and neurodegenerative diseases such as SZ and AD. This could be particularly relevant in therapeutic approaches for preventing or slowing down neurodegenerative processes associated with schizophrenia.

It would also be valuable to clinically assess the longitudinal expression of ErbB4 in SZ patients to determine if expression increases with age and if symptoms worsen with the variable ErbB4 expression. Furthermore, individuals diagnosed with SZ face a markedly elevated risk, approximately 2–4 times higher than that of the general population, for the development of Alzheimer's disease (AD) and other types of dementia (Kochunov et al., 2021). Considering the increased susceptibility of individuals with SZ to AD,

understanding the intricate relationship between ErbB4 expression, neurodegenerative processes, and the progression of both SZ and AD may offer crucial insights for developing 1) biomarkers for the early detection and diagnosis of SZ and AD or 2) targeted therapeutic strategies and interventions.

Final Thoughts

In summary, our investigation into ErbB4 expression in the cortex of control and schizophrenic donors revealed several noteworthy differences. The comparison of ErbB4+ cell counts demonstrated a substantially higher count for experimental specimens, although an outlier influenced this. Upon excluding the outlier, control specimens exhibited higher ErbB4 expression levels, contrasting with prevailing literature that explicates increased ErbB4 expression in schizophrenia. Analysis of cell size displayed variations in morphology, with control specimens exhibiting a larger mean cell size. Additionally, there were observable differences in the distribution of ErbB4+ cells throughout the cortical layers by size and circularity, suggesting distinct cellular characteristics between the SZ and non-SZ groups. The assessment of Feret

angles further highlighted differences in the orientation of ErbB4+ cells for SZ and non-SZ individuals. Taken together, these findings contribute to our understanding of ErbB4+ cell frequency and morphology in schizophrenia while emphasizing the need for further empirical research into its complex role in the pathophysiology of the disorder.

References

- Allen Institute for Brain Science (2013). Technical White Paper: *In Situ* Hybridization in the Allen Human Brain Atlas. Published by Allen Institute. <https://www.semanticscholar.org/paper/allen-human-brain-atlas-technical-white-paper-%3a-in/5fd085020d8f74aaaea84962ced08d7d444b39f3>.
- Chen, Y. J., Zhang, M., Yin, D. M., Wen, L., Ting, A., Wang, P., Lu, Y.S., Zhu, X.H., Li, S.J., Wu, C.Y., Wang, X.M., Lai, C., Xiong, W.C., Mei, L., & Gao, T. M. (2010). Erbb4 in parvalbumin-positive interneurons is critical for neuregulin 1 regulation of long-term potentiation. *Proceedings of the National Academy of Sciences*, 107(50), 21818-21823. <https://doi.org/10.1073/pnas.1010669107>.
- Chong, V.Z., Thompson, M., Beltaifa, S., Webster, M.J., Law, A.J., & Weickert, C.S. (2008). Elevated neuregulin-1 and ErbB4 protein in the prefrontal cortex of schizophrenic patients. *Schizophr Res*. 100(1-3), 270-80. <https://doi.org/10.1016/j.schres.2007.12.474>.
- Correll CU, Solmi M, Croatto G, Schneider LK, Rohani-Montez SC, Fairley L, Smith N, Bitter I, Gorwood P, Taipale H, Tiihonen J. (2022). Mortality in people with schizophrenia: a systematic review and meta-analysis of relative risk and aggravating or attenuating factors. *World Psychiatry*, 21(2):248-271. <https://doi.org/10.1002/wps.20994>.
- Correll, C. U., Bitter, I., Hoti, F., Mehtälä, J., Wooller, A., Pungor, K., & Tiihonen, J. (2022). Factors and their weight in reducing life expectancy in schizophrenia. *Schizophrenia Research*, 250, 67-75. <https://doi.org/10.1016/j.schres.2022.10.019>.
- Corfas, G., Rosen, K.M, Aratake, H., Krauss, R., Fischbach, G.D. (1995). Differential expression of ARIA isoforms in the rat brain. *Neuron*. 14, 103–115.
- Ferreira, T., & Rasband, W. (2012). ImageJ User Guide. Fiji 1.46 R. [https://imagej.net/ij/docs/menus/analyze.html#:~:text=FeretAngle%20\(0%2D180%20degrees\),is%20the%20minimum%20caliper%20diameter](https://imagej.net/ij/docs/menus/analyze.html#:~:text=FeretAngle%20(0%2D180%20degrees),is%20the%20minimum%20caliper%20diameter).
- Joshi, D., Fullerton, J. M., & Weickert, C. S. (2014). Elevated ErbB4 mRNA is related to interneuron deficit in prefrontal cortex in schizophrenia. *Journal of Psychiatric Research*, 53, 125–132. <https://doi.org/10.1016/j.jpsychires.2014.02.014>.
- Kochunov, P., Zavaliangos-Petropulu, A., Jahanshad, N., Thompson, P.M., Ryan, M.C., Chiappelli, J., Chen, S., Du, X., Hatch, K., Adhikari, B., Sampath, H., Hare, S., Kvarta, M., Goldwaser, E., Yang, F., Olvera, R.L., Fox, P.T., Curran, J.E., Blangero, J., Glahn, D.C., Tan, Y., Hong, L.E. (2021). A white matter connection of schizophrenia and Alzheimer's disease. *Schizophr Bull*. 47(1),197-206. <https://doi.org/10.1093/schbul/sbaa078>.

ADVANCED TOPICS & ESSAYS

- Konrad, A., Vucurevic, G., Musso, F., Stoeter, P., Dahmen, N., & Winterer, G. (2008). Erbb4 genotype predicts left frontotemporal structural connectivity in human brain. *Neuropsychopharmacology*, 34(3), 641-650. <https://doi.org/10.1038/npp.2008.112>.
- Law, A., Kleinman, J., Weinberger, D., & Weickert, C. (2006). Disease-associated intronic variants in the erbb4 gene are related to altered erbb4 splice-variant expression in the brain in schizophrenia. *Human Molecular Genetics*, 16(2), 129-141. <https://doi.org/10.1093/hmg/ddl449>.
- Law, A. J., Shannon Weickert, C., Hyde, T. M., Kleinman, J. E., & Harrison, P. J. (2004). Neuregulin-1 (NRG-1) mRNA and protein in the adult human brain. *Neuroscience*, 127(1), 125–136. <https://doi.org/10.1016/j.neuroscience.2004.04.026>.
- Li, B., Woo, R., Mei, L., & Malinow, R. (2007). The neuregulin-1 receptor erb b4 controls glutamatergic synapse maturation and plasticity. *Neuron*, 54(4), 583-597. <https://doi.org/10.1016/j.neuron.2007.03.028>.
- Marenco, S., Geramita, M., van der Veen, J.W., Barnett, A.S., Kolachana, B., Shen, J., Weinberger, D.R., Law, A.J. (2011). Genetic association of ErbB4 and human cortical GABA levels in vivo. *J Neurosci*. 31(32), 11628-32. <https://doi.org/10.1001/10.1523/1529-11.2011>.
- McCutcheon, R. A., Reis Marques, T., & Howes, O. D. (2020). Schizophrenia—an overview. *JAMA Psychiatry*, 77(2), 201. <https://doi.org/10.1001/jamapsychiatry.2019.3360>.
- Mei, L., & Nave, K.A. (2014). Neuregulin-ERBB signaling in the nervous system and neuropsychiatric diseases. *Neuron*, 83(1), 27–49. <https://doi.org/10.1016/j.neuron.2014.06.007>.
- Neddens, J. and Buonanno, A. (2011). Expression of the neuregulin receptor erbb4 in the brain of the rhesus monkey (macaca mulatta). *Plos One*, 6 (11), e27337. <https://doi.org/10.1371/journal.pone.0027337>.
- Nicodemus, K. K., Luna, A., Vakkalanka, R., Goldberg, T., Egan, M., Straub, R. E., & Weinberger, D. R. (2006). Further evidence for association between Erb B4 and schizophrenia and influence on cognitive intermediate phenotypes in healthy controls. *Molecular psychiatry*, 11(12), 1062–1065. <https://doi.org/10.1038/sj.mp.4001878/>.
- Roy, K., Murtie, J., El-Khodori, B., Edgar, N., Sardi, S., Hooks, B., Benoit-Marand, M., Chen, C., Moore, H., O'Donnell, P., Brunner, D., & Corfas, G. (2007). Loss of erbb signaling in oligodendrocytes alters myelin and dopaminergic function, a potential mechanism for neuropsychiatric disorders. *Proceedings of the National Academy of Sciences*, 104(19), 8131-8136. <https://doi.org/10.1073/pnas.0702157104>.

- Shamir, A., Kwon, O.B., Karavanova, I., Vullhorst, D., Leiva-Salcedo, E., Jansen, M.J., & Buonanno, A. (2012). The importance of the NRG-1/ErbB4 pathway for synaptic plasticity and behaviors associated with psychiatric disorders. *J Neurosci* 32, 2988–2997. <https://doi.org/10.1523/1899-11.2012>.
- Stewart, A.J., Patten, S.B., Fiest, K.M., Williamson, T.S., Wick, J.P., & Ronksley, P.E. (2022). 10-Year Trends in health care spending among patients with schizophrenia in Alberta, Canada. *Can J Psychiatry*. 67(9):723-733. <https://doi.org/10.1177/07067437221082885>.
- Tepper, J. M., & Koós, T. (2016). Chapter 8 - GABAergic interneurons of the striatum. *Handbook of Behavioral Neuroscience*, 157–178. <https://doi.org/10.1016/b978-0-12-802206-1.00008-8>.
- Woo, R.S., Lee, J.H., Yu, H.N., Song, D.Y., & Baik, T.K. (2011). Expression of ErbB4 in the neurons of Alzheimer's disease brain and app/PS1 mice, a model of Alzheimer's disease. *Anatomy & Cell Biology*, 44(2), 116. <https://doi.org/10.5115/acb.2011.44.2.116>.